Fatigue performance of laser shock peened Ti6Al4V and Al6061-T6 alloys

Niroj Maharjan[1], Shi Ying Chan[1], Thivyaa Ramesh[1], Puay Nai[2], and Dennise Ardi[1]

[1]Agency for Science Technology and Research
[2]Tyrida International Pte Ltd

September 11, 2020

Abstract

Propagation of fatigue crack in laser shock peened metallic component is retarded by introduction of deep compressive residual stresses during the process. Apart from large compressive residual stress build-up near the surface, surface topography is also significantly altered during laser shock peening. However, a systematic evaluation of the individual effects of residual stresses and surface topography as well as their interaction effects on fatigue crack initiation and growth is still lacking. This study investigates the effect of laser shock peening on near surface properties of Ti6Al4V and Al6061-T6 alloys and how these changes dictate their overall fatigue performance. The results show that both surface residual stresses and surface topography influence the fatigue life of a component. It is found that fatigue life of Ti6Al4V alloy increased by at least 1.28 times after laser shock peening. In contrast, the improvement is minimal for Al6061-T6 alloy due to the surface roughening effect introduced by laser peening which results in early crack initiation and negates the beneficial effect of compressive residual stresses.

Keywords:

Laser shock peening, fatigue, residual stress, surface topography, Ti6Al4V alloy, Al6061-T6 alloy

Introduction

Structural components of an aircraft might fail catastrophically when they are unable to withstand stresses imposed on them during operation. One of the most common modes of failures in aircraft components is fatigue [1] whereby cracking occurs due to repeated or cyclic loading even at conditions below the nominal yield strength of the material. Therefore, various mechanical surface treatments are deployed to increase resistance to crack initiation and growth and prevent premature fatigue failure.

Laser shock peening (LSP) is an emerging surface treatment process which uses laser-induced shock waves to impart compressive residual stresses on a component and enhance its fatigue life. Compared to conventional peening methods like shot peening, the process introduces deep compressive residual stresses, and is highly precise with ability to generate very high strain rates ($>10^6 s^{-1}$) [2]. The technique has been successfully implemented in aircraft turbine fan blades to improve their resistance against foreign object damage [3] as well as in nuclear plants to increase stress corrosion cracking resistance of weldments [4]. Apart from this, it has also found applications in improving fatigue life of automotive parts [5] and as post-processing method in additive manufacturing [6].

Ever since the invention of LSP in 1960s [7], a number of studies have been dedicated to understand its mechanism and potential for industrial applications. Early studies by Peyre and Fabbro [8] established physics behind pressure generation in confined mode and how plasma induced shock wave generates residual

compressive stresses during LSP. With the booming interest in this relatively new technology, a lot of investigations were carried out to understand the effect of LSP-induced residual stress generation on fatigue behavior of various metals [9–12]. All these studies have unanimously shown the unique capability of LSP to improve fatigue life of mechanical components.

It is generally agreed that the improvement in fatigue life is predominantly due to the magnitude, depth distribution and stability of the induced residual stresses and work hardening near the peened surface [13,14]. Presence of compressive residual stresses retards crack growth rate as significantly higher stress levels are required to overcome the energy barrier for crack propagation [3]. Pavan et al. [15] reported a four times increment in fatigue life after LSP than that in pristine components, mainly due to the reduction of fatigue crack growth rate within laser peened areas. Similarly, Tan et al. [9] showed the effectiveness of LSP in suppressing the fatigue crack growth in 2024-T3 aluminum alloys in presence of various preexisting notch configurations. Furthermore, it has been reported that work hardening introduced during LSP delays crack onset and remains quite stable even at high temperatures. Despite residual stress relaxation at high temperature, Altenberger et al. [16] experimentally demonstrated the enhanced fatigue resistance of LSPed Ti6Al4V alloy (>50 MPa than that of unpeened alloy) at temperatures as high as 550°C due to stability of dense dislocation tangles.

The recent investigations in LSP bespeak a residual stress engineering approach to extend fatigue life of critical aging structures by healing early cracks. Smyth et al. [17] recovered the fatigue life of 2024-T351 aluminum sheet containing scratch damage ranging from 50 – 150 μm deep using LSP. They were able to suppress crack growth by introducing beneficial compressive residual stresses, which extended its fatigue life. However, they found that LSP could not inhibit the initiation of cracks at scribe roots. Similarly, Kashaev et al. [18] employed LSP to restore the fatigue life of laser-beam welded AA6056-T6 butt joints with a pre-existing crack to the level of specimens tested in as-welded condition. Sikhamov et al. [19] exhibited healing of initial cracks in AA2024-T3 alloy with a fastener hole due to LSP, which improved fatigue life by increasing the crack growth period. Moreover, the crack closure mechanism induced by LSP in pre-cracked components has been reported by other researchers as well with some even claiming LSP of pre-cracked specimen increases fatigue life by almost 4 times that of unpeened component without any initial crack [20,21].

While all these studies show the retardation of fatigue crack growth after LSP, little attention is paid towards the influence of peening on crack initiation. In addition to the modification in residual stresses, other surface features like roughness, hardness and microstructure also change during LSP. These features are known to alter the fatigue behavior of a material [22–24]. However, the influence of these changes on fatigue performance of laser peened component is often underestimated. More specifically, these changes might have a significant effect on high cycle fatigue condition, where the beneficial effect of LSP is known to be lower than that in low cycle regime [2014 Lin].

In this study, a systematic evaluation of material properties and its effect on fatigue performance during LSP of two metal alloys – Ti6Al4V and Al6061-T6 is performed. These alloys were selected owing to their unique material properties and significance in aerospace industry. LSP brings change in the microstructure, hardness and surface structure of the material being peened, which in turn defines the surface mechanical properties of the alloy. These properties include residual stress, hardness and surface roughness. The combined effect of these properties on fatigue performance is evaluated by performing a repeated four-point flexural test and examining fractured surfaces.

The results indicate that the fatigue performance of a laser peened alloy is a resultant of the effect of presence of compressive residual stresses, grain refinement, plastic deformation and surface topography. The effect of surface topography was particularly significant in Al6061-T6 alloy than in Ti6Al4V alloy which resulted in just a slight fatigue life improvement in Al6061-T6 alloy despite all other changes. The developed understanding could be helpful in developing guidelines for laser peening parameters for different alloys.

Experimental Methodology

Materials used

The study investigated the effect of LSP on two commonly used aerospace metal alloys – Ti6Al4V and Al6061-T6. Ti6Al4V alloy is used to manufacture fan blades in aircraft engines, which are generally prone to foreign object damage. Similarly, Al6061-T6 is used in automotive components as well as in aircraft structures such as wings and fuselage, which are also subject to fatigue damage. The nominal chemical composition of both alloys are shown in Table 1 and their mechanical properties are listed in Table 2. Both alloys were machined into flat coupons with beveled edges according to the BS EN 6072 standard for fatigue testing [25]. The dimensions and geometry of the coupon is shown in Fig. 1.

Table 1. Nominal chemical composition (in wt%) of the alloys used.

	Ti	Al	V	Fe	C	N	O	Si	Cu	Mn	Mg	Cr	Zn
Ti6Al4V	Bal.	5.8	3.9	0.07	0.02	0.02	0.12	-	-	-	-	-	-
Al6061-T6	0.15	Bal.	-	0.7	-	-	-	0.8	0.4	0.15	1.2	0.35	0.25

Table 2. Mechanical properties of the alloys.

	Elastic Modulus (GPa)	Poisson's ratio	Yield strength (at 0.2% offset) (MPa)	Ultimate tensile strength (M
Ti6Al4V	114	0.34	860	980
Al6061-T6	68.9	0.33	276	310

Hosted file

`image1.emf` available at https://authorea.com/users/357153/articles/479844-fatigue-performance-of-laser-shock-peened-ti6al4v-and-al6061-t6-alloys

Fig. 1. Schematic drawing of specimen geometry used in the study.

Laser Shock Peening

The LSP experiments were performed using a high energy Nd:YAG laser (Tyrida YS120-R200A) with 18 ns pulse duration and 1064 nm wavelength at 4 Hz repetition rate. The laser beam spot was circular and had a flat top energy profile. It was focused to a size of 3 mm diameter at the coupon surface using convergent lens. Fig. 2 shows the experimental setup for LSP. The coupon was held with a fixture mounted on a 6-axis robot arm and placed exactly normal to the incident laser beam at focal plane position for peening. A protective black tape overlay was utilized to protect the surface from thermal effects of the laser beam . On top of the protective overlay, a laminar water flow was maintained in order to confine the plasma and increase shock wave pressure.

Hosted file

`image2.emf` available at https://authorea.com/users/357153/articles/479844-fatigue-performance-of-laser-shock-peened-ti6al4v-and-al6061-t6-alloys

Fig. 2. Experimental setup for laser peening trails.

Fig. 3(a) shows the laser peened area. The laser peen pattern was designed to be applied in four steps as shown in Fig. 3(b) to achieve a total coverage of 314%. In order to avoid damage to the surface, the ablative layer was manually removed and a new ablative layer was applied after each step. A peak power density

of 7.86 GW/cm^2 and 4.42 GW/cm^2 was employed for peening of Ti6Al4V coupons and Al6061-T6 coupons respectively. Based on our previous study, these peak power densities resulted in optimum compressive residual stresses on respective alloys. A total of 7 coupons were prepared for each alloy under the same condition for fatigue testing.

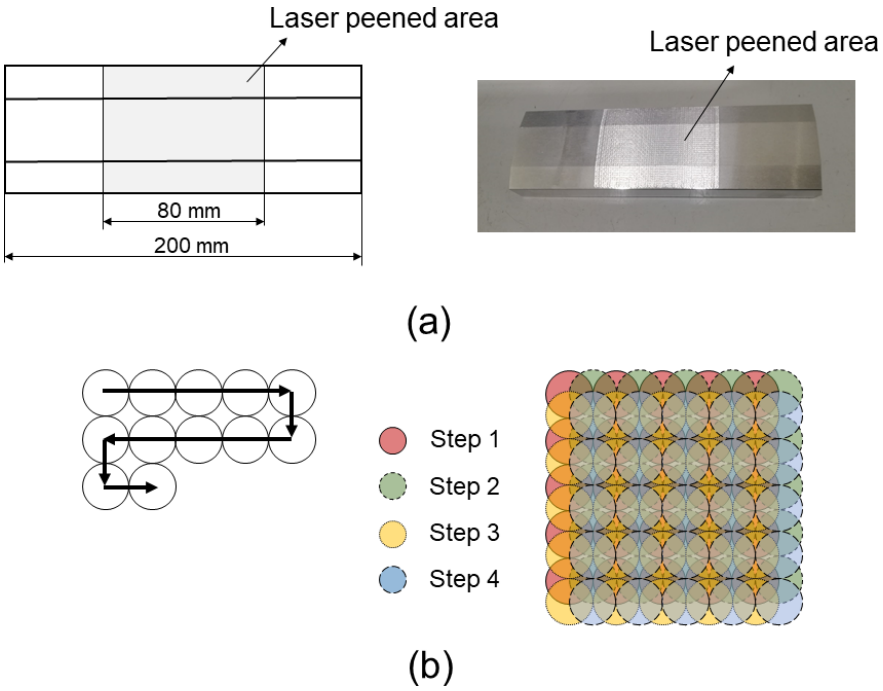

Fig. 3. (a) Image showing laser peened area in the middle section of the specimen; and (b) Four-step LSP toolpath design employed to produced 314% coverage.

Four-point flexural fatigue test

Load controlled four-point flexural fatigue tests were performed using 250 kN MTS Landmark Fatigue Tester. The tests were carried out following ASTM E466 standard [26]. Fig. 4 shows the setup for bend test. The coupons were loaded with the peened surface facing downwards such that the peened region is exposed to maximum bending stresses. The distance between inside rollers were kept at 60 mm and outer rollers at 170 mm gap. Under such configuration, the bending stress experienced by the surface of the coupons (at the largest distance from the neutral axis) can be calculated as:

$$\sigma = \frac{3F(L-L_i)}{2bd^2} \quad (1)$$

where, F is the load being applied, L is the distance between outer roller, L_i is the distance between inner rollers, b is the breadth of the coupons and d is the height of the coupons. The test was performed at the frequency of 10 Hz and R-ratio of 0.1 (tension-tension loading) using sine wave loading. A preload of about 1 kN was applied to the coupons to minimize the movement of coupons during initial cycles of the test. The stress levels were chosen such that the test results were regularly positioned on S-N curve between 10^3 to 10^6 cycles. All coupons were run until to failure or until a runout of 3×10^6cycles was achieved. The obtained data points were fitted in stress vs number of cycles (S-N) curves.

It is interesting to note that four-point bend test is more relevant for fatigue life comparison between peened and unpeened coupons. Compared to three-point bend test which produces peak stress at the mid-section of the coupons, four-point bend test produces peak stresses along an extended region of the coupons surface.

Therefore, a larger volume (in our case, the whole peened surface between two inner rollers) is under stress in four-point bend test which increases the reliability of the results. In addition, it also increases the possibility of identifying the defects and flaws in the peened surface.

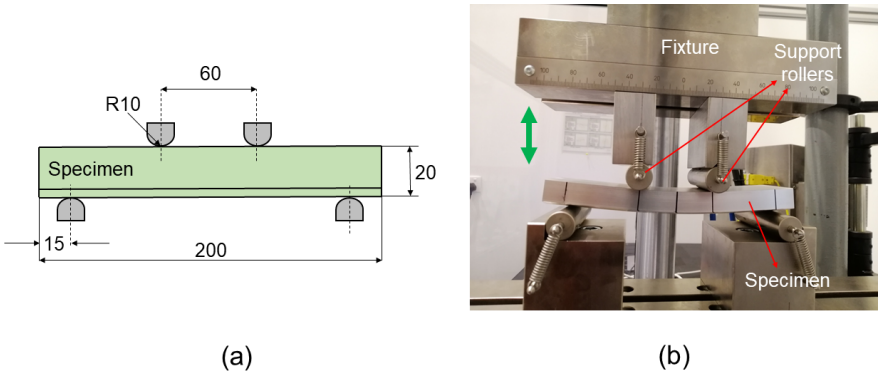

Fig. 4. Four-point flexural fatigue test setup; (a) schematic illustration; and (b) actual setup.

Characterization

After the fatigue test was completed, the broken coupons were cut to a smaller size using electric discharge machining to study the fractured surface. The cut coupons were cleaned with ethanol and dried in air before observing the fractured surface under scanning electron microscope (Carl Zeiss EVO HD).

Other characterization studies were also performed to evaluate the effect of LSP and compare the changes against unpeened coupons. The surface topography was analyzed using a non-contact optimal profilometer based on white light interferometry (Bruker NPFlex). Microhardness measurements were made using Vickers indenter at 100 gf and 10 s dwell time (Innovatest Falcon 500). In order to measure the microhardness variation along the depth, at least five measurements were taken at each depths and the average values are reported. Similarly, cross-section metallographic coupons were prepared following standard sample preparation technique. Ti6Al4V alloy was etched using Kroll's reagent (100 ml distilled water + 5 ml nitric acid + 2 ml HF) and Al6061-T6 was etched under Keller's reagent (95 ml water + 2.5 ml HNO_3+ 1.5 ml HCl + 1.0 ml HF). The etched coupons were observed under an optical microscope (Olympus BX53M) to investigate their microstructure.

For residual stress measurements, incremental centre hole drilling (CHD) technique was employed (SINTech MTS 3000-Restan). The surfaces were gently ground using P600 grit emery paper for strain gauge installation. The surface was then cleaned with Isopropyl alcohol (IPA) and strain gauge rosette was attached to the surface using cyanoacrylate adhesive. The incremental hole drilling was carried out at a drill depth increments of 40 μm, recording the relaxed strains at each increment until it reached a total depth of 1.2 mm. Finally, integral depth method was used to calculate residual stresses from the strain data. The in-plane residual stresses in two directions – longitudinal (σ_1, along the length) and transverse (σ_3, along the width) were reported.

Results and discussion

Surface integrity results

Microstructure

Fig. 5 shows a typical microstructure of as-received and laser peened Ti6Al4V alloy. As-received Ti6Al4V alloy shows the preferential etching of prior β grain boundaries (shown as dotted red line in Fig. 5(a)). The α-platelets (indicated with black arrow heads) could be seen within prior β grains which nucleate from the β grain boundaries via a Widmanstätten transformation [27]. The absence of grain boundary α-phase suggests high cooling rate during alloy production. This is preferred as grain boundary α-phase is deleterious to hot workability of the alloy [28]. An inset image in Fig. 5(a) shows colonies of alpha laths inside a prior β grain, which have needle-like β-phase along lath boundary. After LSP, no significant change could be observed in the microstructure except the fragmentation of needle like β-phase into smaller pieces than in as-received state. The fragmentation of β-phase reduces the volume fraction α-β interface which decreases the resistance to dislocation movement promoting plasticity in the material [29].

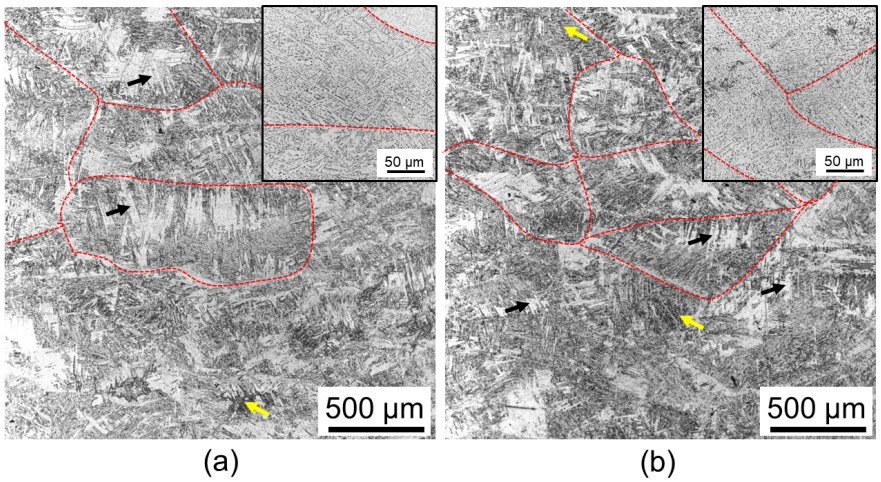

Fig. 5. Typical optical micrographs showing microstructure of (a) as-received; and (b) laser peened Ti6Al4V alloy with high magnification images in insets. The dotted red line indicates prior β grain boundaries. Black and yellow arrows point towards the α-laths and β-phase respectively.

Fig. 6 compares the microstructures of Al6061-T6 alloy before and after LSP. The as-received alloy consisted of large, coarse grains with randomly distributed Mg_2Si-precipitates. These precipitates were formed due to tempering heat treatment. The presence of these precipitates results in hardening of the microstructure. After LSP, the grain size appeared to be reduced. To verify this, the grain size of the alloy before and after LSP was measured using linear intercept method according to ASTM E112 standard [30]. It was found that the grain size reduced from 32 µm to 23 µm after LSP. This indicates grain refinement, which is attributed to the continuous dynamic recrystallization induced by high strain rates of LSP [31]. Strain rates during LSP can go as high as $10^6 s^{-1}$ [32]. At such high strain rates, the dynamic recrystallization process forms new sub-grains owing to the rapid multiplication of dislocation tangles and twin formation produced by severe plastic deformation [31,33]. No particular change in the size and distribution of precipitates was observed.

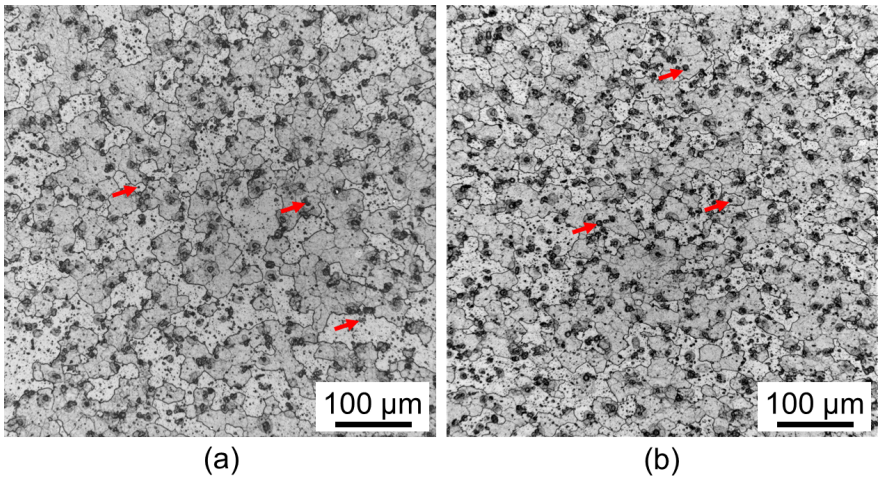

Fig. 6. Optical micrographs of (a) as-received; and (b) laser peened Al6061-T6 alloy. Red arrows show precipitates in the matrix.

Surface topography

Fig. 7 compares the surface topography of as-received and peened Ti6Al4V and Al6061-T6 alloy respectively. It can be seen that the average roughness of Ti6Al4V alloy did not change much after LSP. The as-received Ti6Al4V alloy had an average roughness of about 2 µm, which reduced slightly to about 1.89 µm after LSP. On the contrary, a drastic increment in surface roughness was observed for Al6061-T6 alloy after LSP. The average roughness value increased from 0.71 µm to 8.88 µm. Although both alloys endured battering from laser shocks, the laser peened dimples were more visible in Al6061-T6 alloy than in Ti6Al4V alloy. The peened surface consisted of an array of dimples corresponding to the 4^{th} step peen pattern. This suggests that the final peen pattern has the most significant contribution in determining the surface topology of peened surface.

The higher increment in surface roughness in Al6061-T6 alloy can be attributed to the plastic deformation introduced by high pressure shock waves during LSP. It is inevitable that the plastic deformation occurred in both alloys. However, Al6061-T6, being a softer material, experienced significant deformation than harder Ti6Al4V alloy, which is corroborated by the presence of deeper micro-dents on Al6061-T6 surface. In addition, each peen patterns (from step 1 to step 4) would create a dimple marks on the surface; but only the effect of final peen pattern (step 4) remains visible due to superimposition effect.

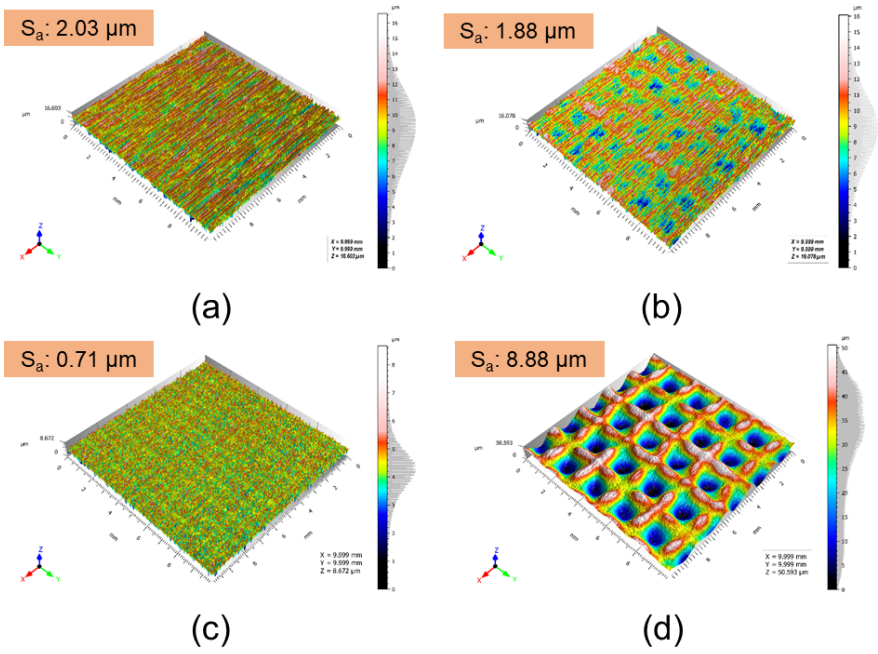

Fig. 7. Surface topography of (a,c) as-received; and (b,d) laser peened Ti6Al4V alloy and Al6061-T6 alloy respectively. The surface roughness increased drastically for laser peened Al6061-T6 alloy compared to Ti6Al4V alloy.

Hardness profile

The hardness of both alloys was also found to increase after LSP. As can be seen from Fig. 8, the microhardness increased by ˜1.2 times and ˜1.4 times for Ti6Al4V alloy and Al6061-T6 alloy respectively. Maximum hardness was recorded at the surface and the value gradually decreased along the depth due to decreasing influence of laser shock waves. Depth of influence higher than 1 mm was achieved for both alloys, which confirms the deeper peening effect of LSP. The increment in hardness can be attributed to the grain refinement and strain hardening due to plastic deformation.

Hosted file

`image8.emf` available at https://authorea.com/users/357153/articles/479844-fatigue-performance-of-laser-shock-peened-ti6al4v-and-al6061-t6-alloys

Fig. 8. Graph comparing the hardness profile of as-received and laser peened alloys.

Residual stresses

One of the main changes brought about by any peening method is the introduction of beneficial compressive residual stresses in near surface region. These stresses originate when a component is stressed beyond its elastic limit. LSP is known to induce deeper and higher compressive residual stresses in the material compared to conventional peening methods [14]. This fact is consolidated by the residual stress results shown in Fig. 9. Both as-received alloys had negligible amount of residual stresses compared to peened cases. It is noteworthy to point out the presence of mild tensile residual stresses in as-received Ti6Al4V alloy. This could be due to the prior-machining step involved in production of Ti6Al4V coupons which induces thermal loading in surface regions.

After LSP, both alloys developed high compressive residual stresses penetrating to a depth higher than 1 mm from the surface. As expected, the depth of penetration was higher for Al6061-T6 than for Ti6Al4V alloy.

On the other hand, a maximum compressive stress of about -600 MPa was recorded for Ti6Al4V alloy at the depth of about 100 μm from the surface, while for Al6061-T6 alloy, the compressive stresses peaked at 145 MPa at the depth of about 180 μm. The lower magnitude of compressive stresses for Al6061-T6 alloy can be attributed to its lower yield strength. Another interesting difference between the two alloys is a higher retention of compressive residual stress between 0.20 mm and 0.60 mm for Al6061-T6 alloy than Ti6Al4V alloy. The reason again boils down to the lower yield strength and high ductility of Al6061-T6 alloy, which allows higher fraction of laser shock wave energy to penetrate deeper into the material. With increasing depth, lesser plastic deformation is generated, resulting in gradual attenuation of compressive residual stress along the depth.

Hosted file

`image9.emf` available at https://authorea.com/users/357153/articles/479844-fatigue-performance-of-laser-shock-peened-ti6al4v-and-al6061-t6-alloys

Fig. 9. Graphs showing variation of residual stresses along the depth for (a) Ti6Al4V alloy; and (b) Al6061-T6 alloy. σ_1 and σ_3 are in-plane residual stresses along longitudinal and transverse directions respectively.

Fatigue performance

Cyclic four-point bend test was performed to evaluate the fatigue performance of the alloys before and after LSP. Fig. 10 shows the S-N curves for both alloys. As can be seen, the S-N curve for peened coupons shifted upwards compared to the unpeened coupons which indicates an improvement in fatigue life after LSP. The endurance limit increased by 1.28 times for Ti6Al4V alloy after LSP. Similarly, fatigue life was found to increase significantly (by two orders of magnitudes) at low stress levels. The S-N curves for Al6061-T6 alloy also show some improvement in fatigue performance after LSP. However, this improvement is not as pronounced as in Ti6Al4V alloy.

Hosted file

`image10.emf` available at https://authorea.com/users/357153/articles/479844-fatigue-performance-of-laser-shock-peened-ti6al4v-and-al6061-t6-alloys

Fig. 10. S-N plots obtained from four-point flexural fatigue test of the alloys. The arrow "?" indicates runout specimens.

The test coupons with typical fracture morphology in each group are shown in Fig. 11. For all coupons, the fracture occurred within the mid-span i.e. in between the two inner rollers, which is the area subjected to maximum bending stress. Multiple micro-cracks were also observed in the mid-region possibly due to the multiple defects near the surface. It can be observed that fracture in Al6061-T6 alloy appears very violent (with a rough topology) compared to Ti6Al4V alloy. The fracture line along the Al6061-T6 surface is also zig-zag compared to Ti6Al4V alloy.

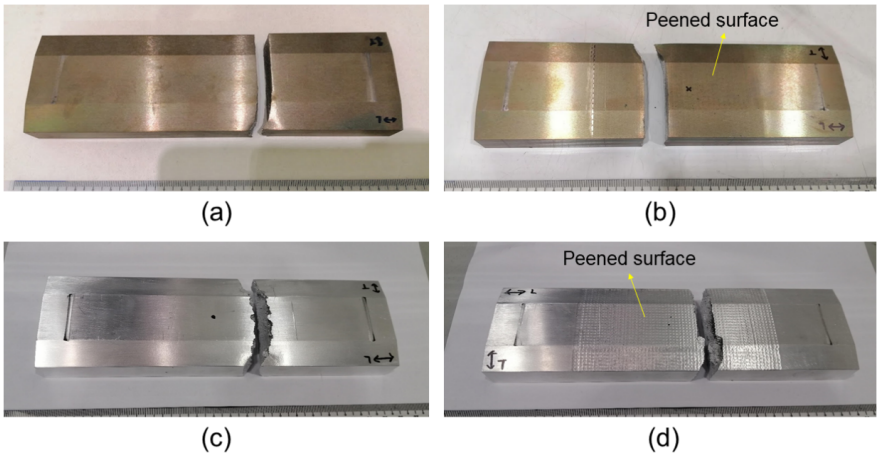

Fig. 11. Photographs showing failure location in (a) as-received and (b) laser peened Ti6Al4V alloy; and (c) as-received and (b) laser peened Al6061-T6 alloy.

Fig. 12 shows the fractured surface of as-received Ti6Al4V alloy under SEM. The fractured surface can be roughly divided into three regions- crack initiation, slow crack growth region and fast fracture (brittle fracture) region. For the as-received coupons, the crack originated from the surface when the load exceeded the fatigue resistance. The surface is generally weak compared to the inner region and is subject to yield. The crack propagates radially in the sub-surface region as seen from the elongated striation marks in slow crack growth region. The striation marks grow further apart as the crack propagates inside the material and a fast brittle fracture occurred which results in complete fracture of the coupons. For LSP-treated coupon the crack initiated in the sub-surface region (see Fig. 13) suggesting surface strengthening due to peening. The slow crack region and the brittle fracture region looks similar to that in as-received coupon as there was no influence of LSP in the bulk of the material.

The fracture surface investigation of Al6061-T6 also revealed similar observations (see Fig. 14 andFig. 15). In case of Al6061-T6, the damaged surface was very rough and therefore, it was challenging to identify the crack initiation site. The cracks initiated near the surface for both as-received and peened coupons.

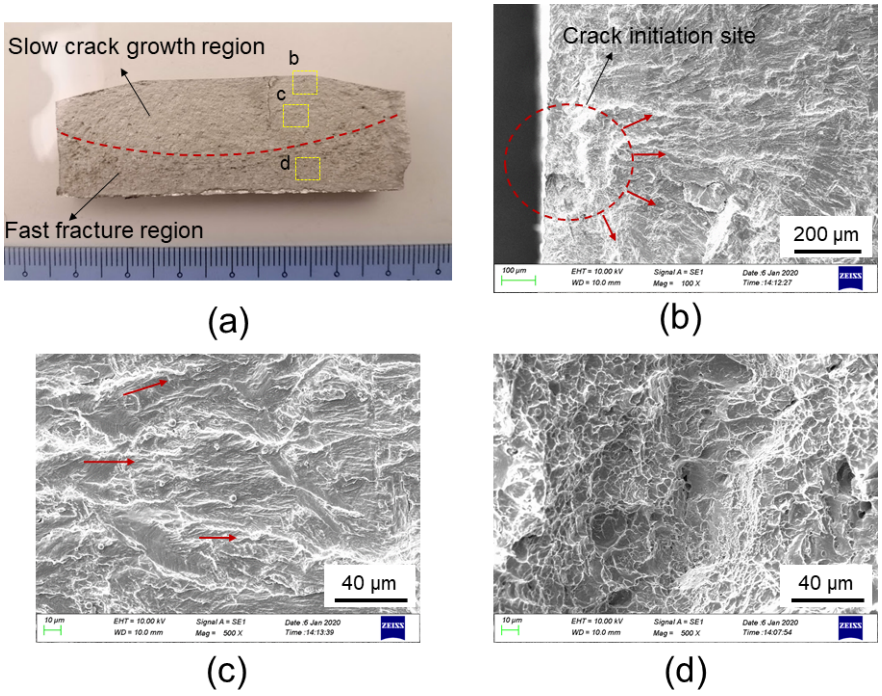

Fig. 12. Fractured surface analysis of as-received Ti6Al4V alloy; (a) fractured surface; (b) crack initiation site; (c) slow crack growth region showing crack propagation direction; and (d) fast fracture region.

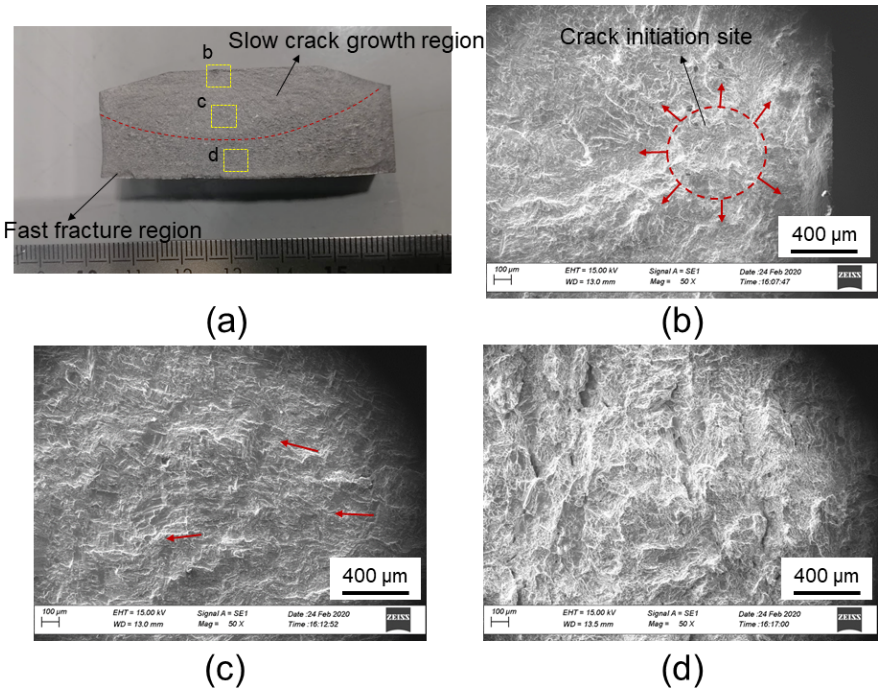

Fig. 13. Fractured surface analysis of laser peened Ti6Al4V alloy; (a) fractured surface; (b) crack initiation site; (c) slow crack growth region; and (d) fast fracture region.

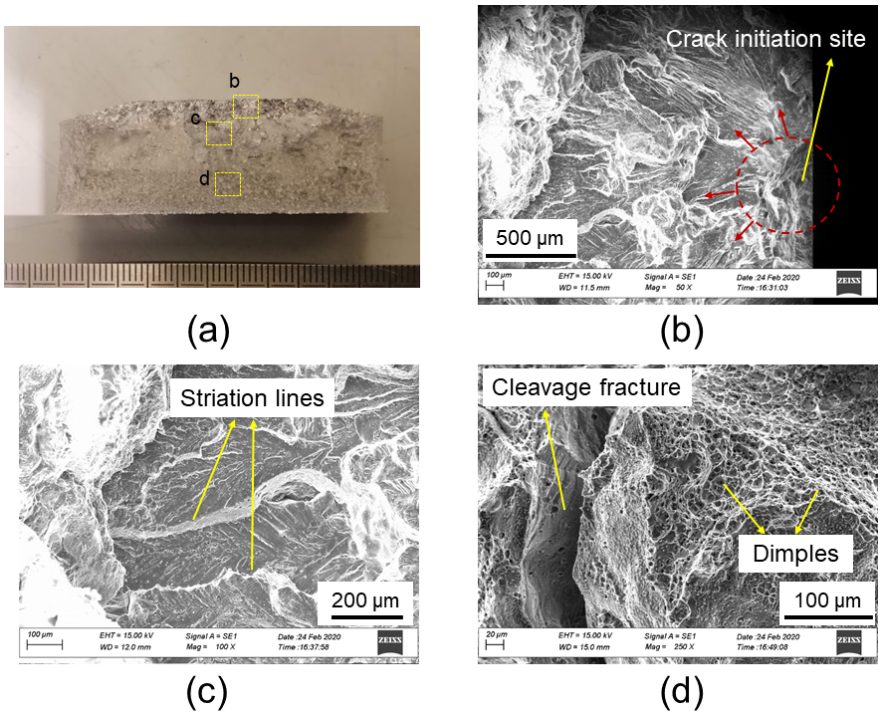

Fig. 14. Fractography of as-received Al6061-T6 alloy; (a) fractured surface; (b) crack initiation site; (c) slow crack growth region; and (d) fast fracture region.

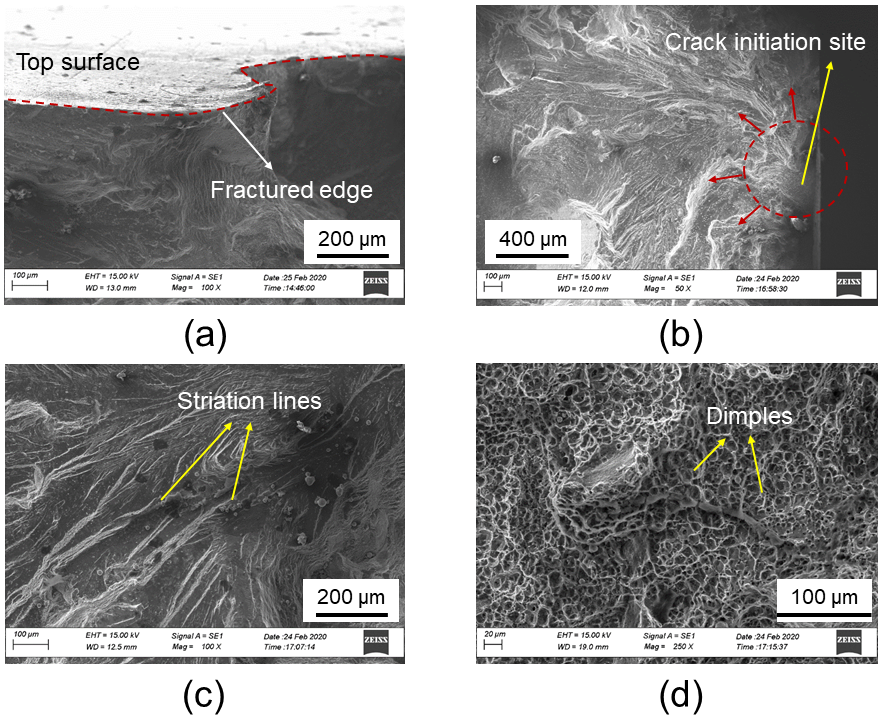

Fig. 15. Fractography of laser peened Al6061-T6 alloy showing (a) fractured edge; (b) crack initiation region;

(c) slow crack growth region; and (d) dimples in fast fracture region.

Discussion

When a high energy pulsed laser beam is focused onto a surface, it results in direct ablation of the surface material [34]. The ablation generates a plasma blow-off which creates a recoil shock wave pressure inside the material. Confinement medium such as water overlay, being transparent to the laser beam, prevents the free expansion of the hot plasma formed due to ablation. As a result, the intensity of shock wave pressure, as well as its duration, is dramatically increased (at least by one order of magnitude for pressure and more than 2 times longer for duration) [8]. Irreversible changes in the structure of material occur in the region where the shock wave pressure exceeds Hugoniot elastic limit of the material [8]. The amplitude of shock wave decreases with the distance from the surface. Its influence can reach as high as 1 mm depth after which the wave becomes weak behaving like a normal acoustic waves.

Our results candidly exhibit that the surface properties of both Ti6Al4V and Al6061-T6 alloys are changed due to the violent change in pressure brought about by laser-induced shock wave. Using TEM investigations, Lainé et al.[2] showed that the high strain rate during LSP generates directional planar dislocations and network of dislocation cells and sub-grains with little or no deformation twinning in Ti6Al4V alloy. This translates to a homogenization of surface microstructure and increase in surface hardness as discussed in Sections 3.1.1 and 3.1.3 respectively. Such work hardened microstructure, comprising of high dislocation density, is reported to delay crack initiation and enhance fatigue strength of the alloy [35]. In addition, our results show that high compressive residual stresses are induced in the surface which extend to 1 mm depth and beyond. The presence of compressive residual stresses aid in crack closure and slows down the crack propagation rate [3]. This suggests that LSP protects Ti6Al4V alloy components from near surface defects and that is the reason why we observed a significant improvement in fatigue life of Ti6Al4V alloy after LSP. The increase in surface strength, not only delayed the onset of crack, but also pushed the crack to initiate from sub-surface region as seen Fig. 13(b).

Compared to the fatigue life improvement for Ti6Al4V alloy, the improvement was marginal for Al6061-T6 alloy although it demonstrated similar changes in surface integrity as in Ti6Al4V alloy. Peyre et al. [36] highlighted that the fatigue improvement in aluminum alloys after LSP is mainly due to the larger increment in crack initiation phase at high cycle fatigue regime. This means that although the peening induces slow crack propagation [21], the presence of large surface defect or asperities can deteriorate the fatigue performance. From our results, a macro-texturing effect is observed on laser peened surface due to severe plastic deformation. This effect was more pronounced in Al6061-T6 alloy than in Ti6Al4V alloy (see Fig. 7) owing to its low yield strength and ductile nature. Compared to the surface roughness achieved in our case, Dhakal and Swaroop [33] achieved a surface roughness of only about 2 μm on Al6061-T6 surface using almost similar peak power density (4 GW/cm^2). However, they used small spot size (0.8 mm) and very high overlap (70%), which accounts for the absence of macro-texturing effect.

The surface dimples act as mini stress raisers causing disruption to stress flow and stresses concentrate in localized regions beneath the dimples (see Fig. 16(a)). As a result, the theoretical stresses increase significantly in the immediate vicinity of such surface irregularities. The effective maximum stress during fatigue loading in presence of surface discontinuities can be quantified as,

$$\sigma_{\max} = K_f \sigma_0 \quad (2)$$

where, σ_0 is the nominal stress and K_f is the fatigue stress concentration factor. The fatigue stress concentration factorK_f is slightly lower than the theoretical stress concentration factor, K_t and is related as,

$$K_f = 1 + q(K_t - 1) \quad (3)$$

where, q is known as the notch sensitivity factor. Notch sensitivity, q can vary from 0 to 1. In absence of any surface irregularities (dimples in this case), q will be zero; thusK_f will be equal to 1. This means there won't be any increase in stress according to equation 2.

For LSPed Al6061-T6 surface, the radius of curvature of dimples was calculated to be about 7.5 mm (see Fig. 16(b)). For such condition, the experimental values for q was obtained from standard chart as 0.82 [37]. The maximum stress concentration occurs at the base of the dimple. Based on the analytical solution for stress concentration factor in sinusoidal shallow surface [38,39], the maximum stress concentration factor, K_t can be related to depth and width of the dimple as

$K_t = 1 + 4\pi\frac{d}{w}$ (4)

This gives us the value of K_t as 1.15. Then, from equation 3, theK_f was calculated to be 1.12. This suggests that the maximum stress at the surface is 1.12 times higher than nominal stresses. For example, if the nominal stress is 400 MPa, the maximum stress can be as high as 448 MPa.

Hosted file

`image16.emf` available at https://authorea.com/users/357153/articles/479844-fatigue-performance-of-laser-shock-peened-ti6al4v-and-al6061-t6-alloys

Fig. 16. Schematic illustration showing (a) imaginary stress flow lines in laser peened coupon; and (b) surface dimples. The undulating peak and valley at the surface generated due to laser peening creates stress concentration regions which negate the beneficial effect of compressive residual stresses and produce lower fatigue life improvements.

From above analysis, it is clear that the beneficial effects on fatigue life introduced by the presence of compressive residual stresses and grain refinement in Al6061-T6 alloy is counterbalanced by the presence of surface irregularities. The initiation of cracks from surface dimples supports this hypothesis. Once the crack is generated, the LSP induced compressive residual stresses delay crack propagation. However, it is not sufficient enough to bring significant increment in fatigue life. Therefore, the overall outcome is just a slight improvement in fatigue life for Al6061-T6 alloy.

The study, thus reveals that the fatigue performance of a LSPed component is determined by a combined effect of both the sub-surface modifications (such as hardness increment, residual stress change, grain refinement) as well as surface asperities. In case of Ti6Al4V alloy, the surface topography showed little change and thus, the improvement in fatigue performance can be primarily attributed to the sub-surface changes. For Al6061-T6 alloy, the surface dimples were found to act as mini stress raisers initiating fatigue crack from the surface and compromising the beneficial effects of sub-surface changes. It is therefore recommended to choose the laser peening parameters such that it creates low surface asperities to achieve significant improvement in fatigue life.

Conclusions

In this study, the influence of laser shock peening on surface integrity and fatigue performance of two commonly used aerospace alloys – Ti6Al4V and Al6061-T6 was experimentally investigated. Based on the analyses, the following conclusions can be drawn:

- LSP is able to generate surface modifications and improve fatigue performance of both alloys. The extremely high strain rates experienced during LSP produces severe plastic deformation near the surface which results in microstructure refinement and introduction of compressive residual stresses near the surface. For Ti6Al4V alloy, hardness increased by approximately 1.2 times and compressive residual stresses as high as -600 MPa was recorded. Similarly, Al6061-T6 alloy after LSP registered a 1.4 times increment in hardness and a maximum compressive residual stress of -150 MPa. The influence of peening extended to a depth of around 1 mm in both alloys.
- The fatigue life of Ti6Al4V alloy increased by more than two orders of magnitude after LSP. This is attributed to the microstructure refinement, hardness increment and presence of deep compressive

residual stresses near the surface. The post-mortem analysis of the fractured surface revealed that LSP strengthened the surface resulting in crack initiation from sub-surface region instead of surface.

- Improvement in fatigue life of LSPed Al6061-T6 alloy was lower compared to that of Ti6Al4V alloy. This is due to the rough surface morphology generated by LSP which increases stress concentration near the surface and diminishes the beneficial effect of compressive stresses.

The study thus shows that both surface morphology and near-surface changes in material properties influence the fatigue performance of an alloy after LSP. It is therefore recommended to select laser peening conditions that can generate the desired microstructure and the required level of compressive residual stresses near the surface without inducing significant change in surface roughness.

Acknowledgement

The authors are grateful to Tyrida International and Advanced Remanufacturing and Technology Centre (ARTC) for providing the funding for this study under research project M19_01_TYR. The authors thank Jolynn Leong for her assistance in managing the project.

References

[1] S.J. Findlay, N.D. Harrison, Why aircraft fail, Mater. Today. 5 (2002) 18–25.

[2] S.J. Lainé, K.M. Knowles, P.J. Doorbar, R.D. Cutts, D. Rugg, Microstructural characterisation of metallic shot peened and laser shock peened Ti–6Al–4V, Acta Mater. 123 (2017) 350–361.

[3] B. Lin, C. Lupton, S. Spanrad, J. Schofield, J. Tong, Fatigue crack growth in laser-shock-peened Ti-6Al-4V aerofoil specimens due to foreign object damage, Int. J. Fatigue. (2014). doi:10.1016/j.ijfatigue.2013.10.001.

[4] Y. Sano, Quarter Century Development of Laser Peening without Coating, Metals (Basel). 10 (2020) 152.

[5] K. Tang, W. Wang, H. Ding, L. Zhou, J. Guo, W. He, Z. Cai, Q. Liu, Z. Zhou, Influence of laser shock peening on fatigue performance of LZ50 axle steel for railway wheel set, Fatigue Fract. Eng. Mater. Struct. (2020).

[6] N. Kalentics, M.O.V. de Seijas, S. Griffiths, C. Leinenbach, R.E. Logé, 3D laser shock peening – A new method for improving fatigue properties of selective laser melted parts, Addit. Manuf. (2020). doi:10.1016/j.addma.2020.101112.

[7] A.H. Clauer, Laser shock peening, the path to production, Metals (Basel). 9 (2019) 626.

[8] P. Peyre, R. Fabbro, Laser shock processing: a review of the physics and applications, Opt. Quantum Electron. 27 (1995) 1213–1229.

[9] Y. Tan, G. Wu, J. Yang, T. Pan, Laser shock peening on fatigue crack growth behaviour of aluminium alloy, Fatigue Fract. Eng. Mater. Struct. 27 (2004) 649–656.

[10] E. Maawad, Y. Sano, L. Wagner, H.G. Brokmeier, C. Genzel, Investigation of laser shock peening effects on residual stress state and fatigue performance of titanium alloys, Mater. Sci. Eng. A. (2012). doi:10.1016/j.msea.2011.12.072.

[11] M. Kattoura, S.R. Mannava, D. Qian, V.K. Vasudevan, Effect of laser shock peening on residual stress, microstructure and fatigue behavior of ATI 718Plus alloy, Int. J. Fatigue. (2017). doi:10.1016/j.ijfatigue.2017.04.016.

[12] S. Prabhakaran, S. Kalainathan, P. Shukla, V.K. Vasudevan, Residual stress, phase, microstructure and mechanical property studies of ultrafine bainitic steel through laser shock peening, Opt. Laser Technol. (2019). doi:10.1016/j.optlastec.2019.02.041.

[13] C.S. Montross, T. Wei, L. Ye, G. Clark, Y.-W. Mai, Laser shock processing and its effects on microstructure and properties of metal alloys: a review, Int. J. Fatigue. 24 (2002) 1021–1036.

[14] K. Ding, L. Ye, Laser shock peening: performance and process simulation, Woodhead Publishing, 2006.

[15] M. Pavan, D. Furfari, B. Ahmad, M.A. Gharghouri, M.E. Fitzpatrick, Fatigue crack growth in a laser shock peened residual stress field, Int. J. Fatigue. (2019). doi:10.1016/j.ijfatigue.2019.01.020.

[16] I. Altenberger, R.K. Nalla, Y. Sano, L. Wagner, R.O. Ritchie, On the effect of deep-rolling and laser-peening on the stress-controlled low- and high-cycle fatigue behavior of Ti-6Al-4V at elevated temperatures up to 550 °c, Int. J. Fatigue. (2012). doi:10.1016/j.ijfatigue.2012.03.008.

[17] N.A. Smyth, M.B. Toparli, M.E. Fitzpatrick, P.E. Irving, Recovery of fatigue life using laser peening on 2024-T351 aluminium sheet containing scratch damage: The role of residual stress, Fatigue Fract. Eng. Mater. Struct. (2019). doi:10.1111/ffe.12981.

[18] N. Kashaev, D. Ushmaev, V. Ventzke, B. Klusemann, F. Fomin, On the application of laser shock peening for retardation of surface fatigue cracks in laser beam-welded AA6056, Fatigue Fract. Eng. Mater. Struct. (2020). doi:10.1111/ffe.13226.

[19] R. Sikhamov, F. Fomin, B. Klusemann, N. Kashaev, The influence of laser shock peening on fatigue properties of AA2024-T3 alloy with a fastener hole, Metals (Basel). (2020). doi:10.3390/met10040495.

[20] K. Takahashi, Y. Kogishi, N. Shibuya, F. Kumeno, Effects of laser peening on the fatigue strength and defect tolerance of aluminum alloy, Fatigue Fract. Eng. Mater. Struct. (2020). doi:10.1111/ffe.13201.

[21] Y. Hu, H. Cheng, J. Yu, Z. Yao, An experimental study on crack closure induced by laser peening in pre-cracked aluminum alloy 2024-T351 and fatigue life extension, Int. J. Fatigue. (2020). doi:10.1016/j.ijfatigue.2019.105232.

[22] M. Suraratchai, J. Limido, C. Mabru, R. Chieragatti, Modelling the influence of machined surface roughness on the fatigue life of aluminium alloy, Int. J. Fatigue. (2008). doi:10.1016/j.ijfatigue.2008.06.003.

[23] D. Novovic, R.C. Dewes, D.K. Aspinwall, W. Voice, P. Bowen, The effect of machined topography and integrity on fatigue life, Int. J. Mach. Tools Manuf. 44 (2004) 125–134.

[24] G.Q. Wu, C.L. Shi, W. Sha, A.X. Sha, H.R. Jiang, Effect of microstructure on the fatigue properties of Ti–6Al–4V titanium alloys, Mater. Des. 46 (2013) 668–674.

[25] British Standard, Aerospace series - Metallic materials - Test methods - Constant amplitude fatigue, UK, 2010.

[26] ASTM E466, Practice for conducting force controlled constant amplitude axial fatigue tests of metallic materials, ASTM B. Stand. (2015). doi:10.1520/E0466-15.2.

[27] R. Pederson, Microstructure and phase transformation of Ti-6Al-4V, (2002).

[28] L. Guo, X. Fan, G. Yu, H. Yang, Microstructure control techniques in primary hot working of titanium alloy bars: A review, Chinese J. Aeronaut. 29 (2016) 30–40.

[29] G. Lütjering, J.C. Williams, A. Gysler, Microstructure and mechanical properties of titanium alloys, in: Microstruct. Prop. Mater. (Volume 2), 2000: pp. 1–77.

[30] ASTM E112-13 Standard Test Methods for Determining Average Grain Size, (2013).

[31] J.Z. Zhou, S. Huang, J. Sheng, J.Z. Lu, C.D. Wang, K.M. Chen, H.Y. Ruan, H.S. Chen, Effect of repeated impacts on mechanical properties and fatigue fracture morphologies of 6061-T6 aluminum subject to laser peening, Mater. Sci. Eng. A. (2012). doi:10.1016/j.msea.2012.01.125.

[32] W. Braisted, R. Brockman, Finite element simulation of laser shock peening, Int. J. Fatigue. 21 (1999) 719–724.

[33] B. Dhakal, S. Swaroop, Effect of laser shock peening on mechanical and microstructural aspects of 6061-T6 aluminum alloy, J. Mater. Process. Technol. 282 (2020) 116640.

[34] N. Maharjan, W. Zhou, Y. Zhou, Y. Guan, N. Wu, Comparative study of laser surface hardening of 50CrMo4 steel using continuous-wave laser and pulsed lasers with ms, ns, ps and fs pulse duration, Surf. Coatings Technol. 366 (2019). doi:10.1016/j.surfcoat.2019.03.036.

[35] X.C. Zhang, Y.K. Zhang, J.Z. Lu, F.Z. Xuan, Z.D. Wang, S.T. Tu, Improvement of fatigue life of Ti-6Al-4V alloy by laser shock peening, Mater. Sci. Eng. A. (2010). doi:10.1016/j.msea.2010.01.076.

[36] P. Peyre, R. Fabbro, P. Merrien, H.P. Lieurade, Laser shock processing of aluminium alloys. Application to high cycle fatigue behaviour, Mater. Sci. Eng. A. (1996). doi:10.1016/0921-5093(95)10084-9.

[37] G. Sines, J.L. Waisman, T.J. Dolan, Metal fatigue, McGraw-Hill, 1959.

[38] H. Gao, Stress concentration at slightly undulating surfaces, J. Mech. Phys. Solids. 39 (1991) 443–458.

[39] H. Medina, A stress-concentration-formula generating equation for arbitrary shallow surfaces, Int. J. Solids Struct. 69 (2015) 86–93.

Hosted file

`01 Specimen design.pptx` available at https://authorea.com/users/357153/articles/479844-fatigue-performance-of-laser-shock-peened-ti6al4v-and-al6061-t6-alloys

Hosted file

`02 Schematics.pptx` available at https://authorea.com/users/357153/articles/479844-fatigue-performance-of-laser-shock-peened-ti6al4v-and-al6061-t6-alloys

Hosted file

`03 LSP Pattern.pptx` available at https://authorea.com/users/357153/articles/479844-fatigue-performance-of-laser-shock-peened-ti6al4v-and-al6061-t6-alloys

Hosted file

`04 Fatigue test setup.pptx` available at https://authorea.com/users/357153/articles/479844-fatigue-performance-of-laser-shock-peened-ti6al4v-and-al6061-t6-alloys

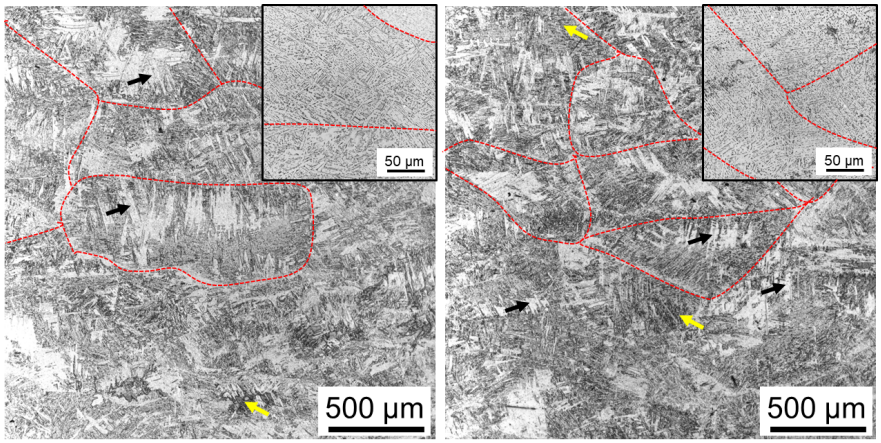

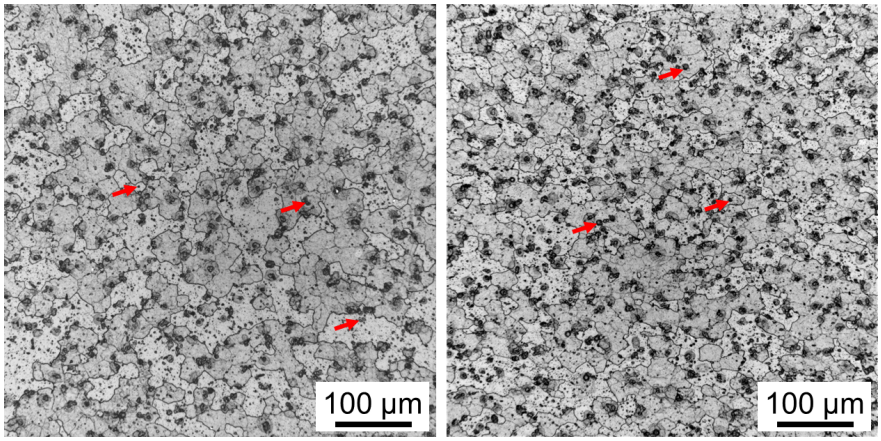

Hosted file

07 Surface topography.pptx available at https://authorea.com/users/357153/articles/479844-fatigue-performance-of-laser-shock-peened-ti6al4v-and-al6061-t6-alloys

Hosted file

08 Hardness.pptx available at https://authorea.com/users/357153/articles/479844-fatigue-performance-of-laser-shock-peened-ti6al4v-and-al6061-t6-alloys

Hosted file

09 RS.pptx available at https://authorea.com/users/357153/articles/479844-fatigue-performance-of-laser-shock-peened-ti6al4v-and-al6061-t6-alloys

Hosted file

10 SN curve.pptx available at https://authorea.com/users/357153/articles/479844-fatigue-performance-of-laser-shock-peened-ti6al4v-and-al6061-t6-alloys

Hosted file

11 Fractured samples.pptx available at https://authorea.com/users/357153/articles/479844-fatigue-performance-of-laser-shock-peened-ti6al4v-and-al6061-t6-alloys

Hosted file

12 Fractography-Ti64 as received.pptx available at https://authorea.com/users/357153/articles/479844-fatigue-performance-of-laser-shock-peened-ti6al4v-and-al6061-t6-alloys

Hosted file

13 Fractography-Ti64 LSPed.pptx available at https://authorea.com/users/357153/articles/479844-fatigue-performance-of-laser-shock-peened-ti6al4v-and-al6061-t6-alloys

Hosted file

14 Fractography-Al6061-T6 as received.pptx available at https://authorea.com/users/357153/articles/479844-fatigue-performance-of-laser-shock-peened-ti6al4v-and-al6061-t6-alloys

Hosted file

15 Fractography-Al6061-T6 LSPed.pptx available at https://authorea.com/users/357153/articles/479844-fatigue-performance-of-laser-shock-peened-ti6al4v-and-al6061-t6-alloys

Hosted file

16 Stress raisers.pptx available at https://authorea.com/users/357153/articles/479844-fatigue-performance-of-laser-shock-peened-ti6al4v-and-al6061-t6-alloys